Journal of Machine Engineering, 2019, Vol. 19, No. 3, 17–30
ISSN 1895-7595 (Print) ISSN 2391-8071 (Online)

Received: *07 January 2019* / Accepted: *30 May 2019* / Published online: *25 September 2019*

finite-element-method, reinforced concrete,
thermal solid simulation, temperature field

Janine GLÄNZEL[1]
Alexander GEIST[1*]
Steffen IHLENFELDT[1,2]

SIMULATION-BASED INVESTIGATION FOR HEAT TRANSFER BEHAVIOR OF STEEL REINFORCEMENTS IN CONCRETE MACHINE FRAMES AND THEIR THERMAL EFFECTS

The determination of the thermal-elastic behavior is one of the main aspects in the design phase of new machine frames. Prototypically simulation models are used for preliminary investigations, which are based on finite element approaches and usually work with simplified material laws. By the manufacturing of machine frames of concrete steel reinforcements are used to ensure the operation reliability due to the high sensitivity of concrete to tensile stresses. Because of different thermal conductivity and specific heat capacity of steel and concrete the reinforcement has a not negligible influence on the total thermal behavior of the system, which cannot be covered with conventional material laws, e.g. from material libraries. Preliminary investigations show, that a volume fraction more than 1 % of the reinforcement of the total volume can cause a relative error up to ten percent in the temperature field. To reflect the real behavior of reinforced concrete for a machine bed, the influence should be exanimated for two different approaches. Next to the real illustration of the geometry of the reinforcement in the FE-model, decoupled simulation approaches are used on reduced models, which should approach numerically the material behavior of the reinforcement.

1. INTRODUCTION

Thermal measurements on machine tools show repeatedly that despite the thermo-symmetrical design it is not possible to achieve a uniform temperature distribution. Feasible causes are drives arranged on symmetrical structures on one side, external heat sources such as solar radiation or machine waste heat or locally varying processes in the working space [1, 2]. These local or area wide heat inputs can have a significant influence on the resulting deformation behavior of the machine tool structure, e. g. the machine frame [3, 4]. In order to compensate for this effect and the resulting TCP shift, the heat must be dissipated as efficiently as possible. For this purpose, cooling circuits are usually integrated into active components and passive structures, which are usually adapted to the temperature of the structure [5]. The use of high performance concrete (HPC) in casting opens up

[1] Fraunhofer Institute for Machine Tools and Forming Technology IWU, Chemnitz, Germany
[2] Dresden University of Technology TUD, Dresden, Germany
[*] E-mail: Alexander.Geist@iwu.fraunhofer.de
https://doi.org/10.5604/01.3001.0013.4077

completely new possibilities for the integration of cooling channel structures for an active temperature control [6].

In order to reduce thermally induced displacements, EPUCRET has carried out an appropriate temperature control of concrete frame structures. Initially, simple prismatic bodies were measured under defined thermal stress series in order to be able to independently adjust the cooling system from the central control unit. For example, the straightness of guide rails has been reduced from ±35 μm to ±2 μm. In subsequent tests, this approach was applied to complete machine tools, where several individual circuits are coupled or work separately. The most important TCP shifts were measured and reduced by at least 50%. In this context, energy aspects have not been taken into account [7] and transferability to other systems is not known.

As the example DMG MORI [8] shows, structurally integrated cooling circuits are already established. These stabilize precision-relevant components, such as the machine bed or the gantry, but also linear guides and drives. In this way, the heat input from internal heat sources can be dissipated, which leads to an improvement of the thermal behavior.

The aim is to present the methodological approach for the simulation-technical analysis and optimization of cooling systems in machine tool frames made of HPC.

This paper is intended to provide an overview of modelling the thermal influence between the composite materials of concrete and steel. Because of different thermal conductivity and specific heat capacity of steel and concrete the reinforcement has a not negligible influence on the total thermal behavior of the system, which cannot be covered with conventional material laws, e. g. from material libraries. Therefore in Chapter 2 some theoretical basics for modelling the heat conduction will be discussed. Subsequently in Chapter 3 the simulation approach for the reinforcement follows by describing the material model of the composite material. The material model modified the important parameters, e.g. thermal conductivity and the heat capacity. Last but not least in Chapter 4 the transfer of the method on a real machine frame will be presented.

2. THEORETICALLY BASICS OF A THERMAL SOLID BODY SIMULATION AND USAGE

At first it will be considered an shortly extract of theoretical basics for describing the thermal-effects of a solid body and modelling of material behavior. The physical context of the heat conduction in a solid body is given by the heat equation [9].

This analytical parabolic partial differential equation is given in form:

$$\frac{\partial T}{\partial t} = a\Delta T \tag{1}$$

with: $a = \lambda/(\rho\ c)$ is valid for the unsteady temperature field T without internal heat sources.

The coefficient a is the thermal diffusivity. This important parameter is a quotient of the thermal conductivity λ and the product of the density ρ and specific heat capacity c. All parameter are constant in time t, because their dependence of the temperature T are negligible e.g. for the material steel and concrete, in a temperature range of 20 to 100 Celsius degree.

This equation (1) is analytically only for simple problems like a plane wall, a pipe or a sphere, where a 1D-problem is present, solvable [9]. For complex geometrical bodies this equation can only be solved with numerical methods, for example with the finite-element-(FE)-method [9]. In course of this the complex geometry is separated in elementary FE-elements, where the equation is set up for the three coordinates (x, y, z) in 3D of the temperature field. For all three directions the heat transfer equation system (2) is written for a piecewise constant a by:

$$\frac{\partial T_i}{\partial t} = a\left(\frac{\partial^2 T_i}{\partial x^2} + \frac{\partial^2 T_i}{\partial y^2} + \frac{\partial^2 T_i}{\partial z^2}\right), \tag{2}$$

with: $i = 1\ldots N$ (number of volume elements).

The system of equations can only be solved for small time steps t_i ($n = 1\ldots t_n$) explicit, that means in a direct way for every time step t_i in dependence with the previous step. For larger time steps the solution has to be calculated iterative for each time step. The advantage of iterative methods is the high stability for large time steps by little increased calculation time. This method is used usually by thermal problems, where slowly temperature processes take place, e.g. on thermal sluggish constructions like machine frames. Common FEM-solutions like ANSYS 18.1 on the market usually chose the type of solver controlled by the software, which make them highly user friendly.

The context between a heat flux $\dot{q}$ and the heat conduction λ is connected by the law of Fourier (3):

$$\dot{q} = -\lambda \operatorname{grad} T \tag{3}$$

The thermal conductivity coefficient λ as a constant size defines the rate of the temperature gradient, the heat flux density $\dot{q}$ describes the resulting vector field. A high thermal conductivity means a more homogeneous temperature field T in the solid body, because of the better conduction of the heat through the solid body. On the other hand the specific heat capacity c and the density ρ determine which amount of energy is necessary to reach a certain level of temperature in a body. On the other hand a high heat capacity or density means that more time is needed to reach the steady state. The conflict is shown in the Fig. 1.

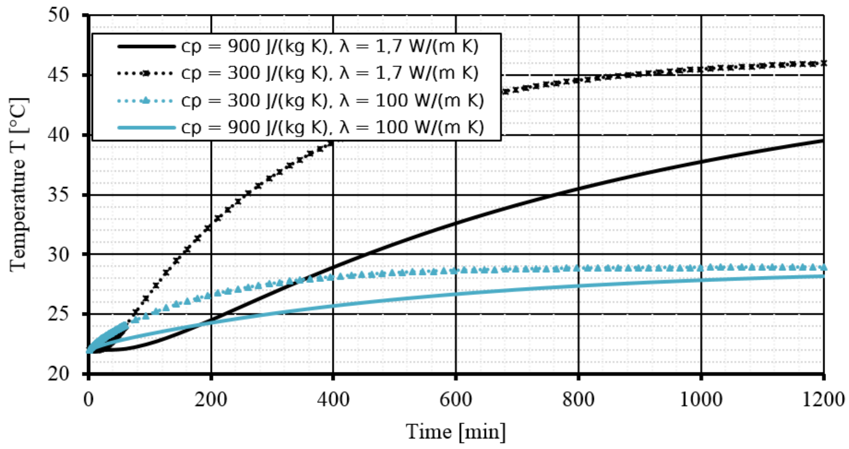

Fig. 1. Influence of the thermal heat conduction and specific heat capacity to the temperature field

In this Fig. 1 the physically context is shown between the thermal conduction λ and the heat capacity c. The trend of the curves is based on an unsteady simulation by a simplified model of a rectangular solid, which is described in the fourth chapter in more detailed.

3. APPROXIMATION METHODS OF MATERIAL COEFFICIENTS

The descripted analysis in Chapter 2 is only valid for homogenous material of solid bodies with a direction-independent thermal conductivity λ. Composite materials, which are used for the production of machine frames, cannot be modelled by analytical basics. In this case thermal conductivity depends from the direction of the different materials and cannot be calculated correctly enough by using the basic equations. The challenge is now to find an approximately way to calculate the composite material of concrete and reinforced steel, which is used e.g. for machine frames. Table 1 shows the highly different thermal behaviour of steel and concrete.

Table 1. Thermal material properties for steel and concrete

	Specific heat capacity [J/(kgK)]	Density [kg/m³]	Heat conduction coefficient [W/(mK)]
steel (S235JR)	461	7850	54
high performance concrete	900	2400	1.7

Consequently in the simulation models the material dependence have to be considered from a certain volume fraction from steel in the concrete. Otherwise the material error has a too big influence on the solution accuracy. Approximation of the searched coefficient for the thermal material behaviour of composite material is modelled by using the numerical approach of the finite element method. Considering of the composite material effects in the calculation model is offered the following opportunities:

I. Implementation of the steel reinforcement as a real 3D solid body.
II. Implementation of the steel reinforcement as 1D line bodies in the geometry.
III. Definition of the material data as a function of the local position $\{c, \rho, \lambda\}:\rightarrow f(\vec{r})$ (4)
IV. Determination of equivalent material data on reduced models. These modified values of material properties are transferred to a homogenous body.

The first method has the highest grade of details, because the reinforcement is implemented as a 3D-CAD-model. The heat transfer is ideal on a federated contact between the steel and concrete (thermal contact resistance is zero). For this aspect a fine mesh on the contact area is necessary, the number of elements and nodes increases rapidly. Because of the high calculation time and memory consumption this method is not practicable. A reduction of the element number can be accomplished with the second method, where the steel reinforcement is placed as a system of 1D line bodies. This decreases the calculation time a little bit. At least there is still an amount of elements because of the complex concrete geometry. The third method does not increase the calculation time because the volume can be meshed as a homogeneous solid body. In opposite, there is a mathematical effort for the description of the material data. The last method is based on a homogeneous solid body with modified values for the thermal conduction and the specific heat capacity to approximately consider the reinforcement. For this method the volume fraction of the reinforcement has to be estimated from the total volume. By the help of reduced models with different spacing of the reinforcement the thermal behavior can be estimated with simulations. The additionally modelling and calculation effort is noticeably lower than the first described method.

4. MODELLING APPROACH FOR THE REINFORCEMENT INFLUENCE ON SIMPLIFIED MODEL

By using the approach to approximate the material coefficient at first it is modelled on a simplified model. Subsequently the calculation effort and the number of elements keep an acceptable level for fast iterative FE calculations. The most primitive construction is a rectangular solid with an equidistant and variable spacing of the reinforcement in each space direction. Therefore a FE-model of rectangular solids inclusive different grids of reinforcement is created. The combination parts of steel and concrete are variate in four cases, which can be considered in Fig. 2.

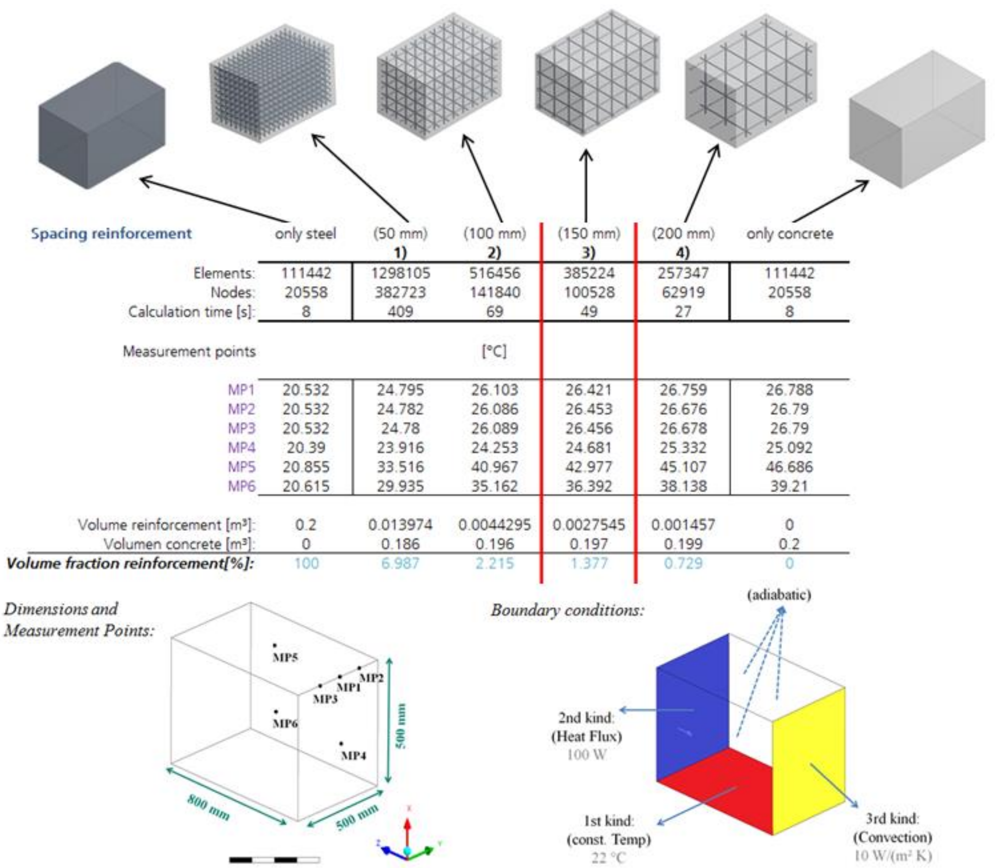

Spacing reinforcement	only steel	(50 mm) 1)	(100 mm) 2)	(150 mm) 3)	(200 mm) 4)	only concrete
Elements:	111442	1298105	516456	385224	257347	111442
Nodes:	20558	382723	141840	100528	62919	20558
Calculation time [s]:	8	409	69	49	27	8
Measurement points			[°C]			
MP1	20.532	24.795	26.103	26.421	26.759	26.788
MP2	20.532	24.782	26.086	26.453	26.676	26.79
MP3	20.532	24.78	26.089	26.456	26.678	26.79
MP4	20.39	23.916	24.253	24.681	25.332	25.092
MP5	20.855	33.516	40.967	42.977	45.107	46.686
MP6	20.615	29.935	35.162	36.392	38.138	39.21
Volume reinforcement [m³]:	0.2	0.013974	0.0044295	0.0027545	0.001457	0
Volumen concrete [m³]:	0	0.186	0.196	0.197	0.199	0.2
Volume fraction reinforcement[%]:	100	6.987	2.215	1.377	0.729	0

Fig. 2. Reduced model for the investigation of the reinforcement

The spacing of the reinforcement as a free parameter in the model should match with the spacing in the real body as much as possible. For the investigation of the context between the volume fraction of the reinforcement and the thermal behaviour, four different common sizes of spacing are set. These chosen sizes of spacing are 50 mm, 100 mm, 150 mm and 200 mm. The both extreme limits are a whole body of concrete or steel. The reinforcement has a diameter of 10 mm. The choice of the boundaries is referenced to the location of a tool machine (see Fig. 2). On the left side there is a heat flux of 100 W on the whole area, this mean a heat flux density of 400 W/m². A constant temperature of 22°C is defined on the bottom area, which represents the install area and the ground temperature. On the right side there is a convection boundary with an environmental temperature of 23°C and a heat transfer coefficient of 10 W/(m K). All other areas are defined as adiabatic. The heat flux proceeds from the left side to right side through the solid body and is influenced by the bottom temperature. Finally the waste heat goes to the environment by convection. Six virtual temperature measurement points are defined in the middle of the body (MP5) or on the surface as references point for the evaluation of the results. MP4 (top) and MP1 (middle) are placed on the area for the convection. The both measurement points MP2 and MP3 are for checking the mesh quality, because they have to own the same values in cause of the symmetry.

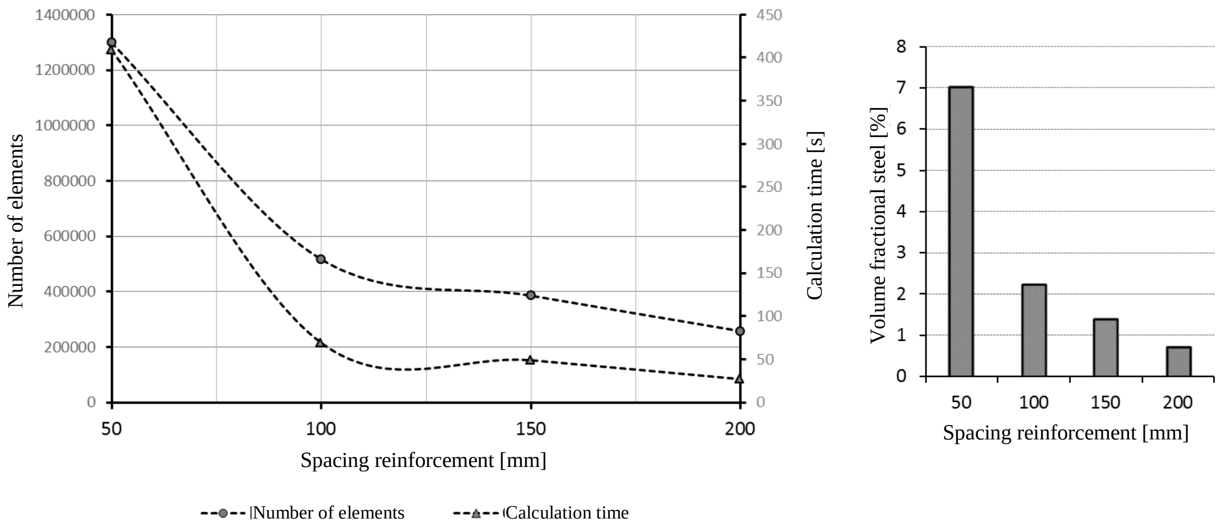

Fig. 3. Dependence of the model behaviour from the spacing of the reinforcement

During the mixing process of different mesh densities have been investigated to keep the meshing error as low as possible but at least to reach a low calculation time. Because of the complex geometry a tetrahedral-mesh-algorithm has been used in the commercial Software Ansys 18.1. The result is shown in the Fig. 4.

The mesh with intermediate refinement was the best compromise between calculation velocity and accuracy. The temperature error between the six measurement points with a fine mesh is below 1%. Consequently this mesh can be used for further calculations. The comparison off all investigated meshes in terms of calculation time is shown in the Table 2 (spacing: 50 mm).

Table 2. Comparison of the element count and the calculation time

	Very coarse	Medium	Fine	Very fine	Prism layer
Elements	50204	156583	657256	2468826	1346435
Nodes	13598	39738	144333	472931	385065
Calculation time [s]	9	19	61	224	109

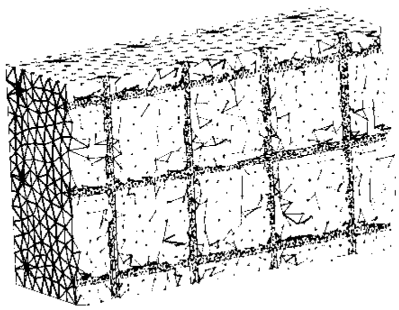

Fig. 4. Optimal mesh configuration

For identifying the temperature field in the simplified model it is necessary to perform a steady state and a transient FE-simulation. The reference values of the points MP1 and MP6 are used for the verification of the calculated temperature fields which depend of the reinforcement ratio. These are the basement for comparison of the approximation model with homogenous material. Figure 5 shows a study of the element density of the FE-mesh refinement. Two cases of mesh refinement have been investigated. Therefore the two meshes present the FE-model with the reinforced spacing of 150 mm. For the coarse meshed case is recognizable that the finite elements are irregular distributed. This adverse aspect is reflected in the resulting temperature field on the right side of Fig. 6. The result for the fine meshed FE-model is finer dissolved as the coarse meshed FE-model. Certainly the finer mesh needs a higher performance time, which is not negligibly for geometrical complex models. Then it is the challenge to find a mesh refinement which is fine enough and leads to sufficient simulation results with acceptable performance time.

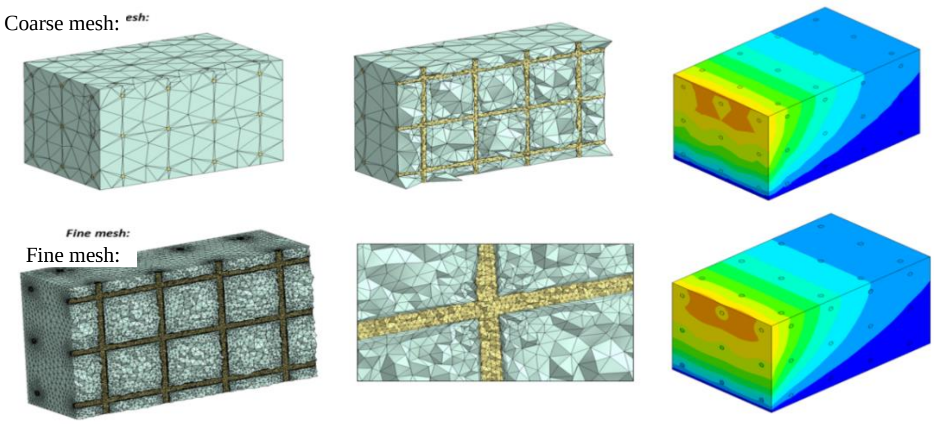

Fig. 5. Comparison of the element density

The FE-simulation can be start after determination of the mesh refinement and the definition of the boundary conditions. Therefore the stationary and the transient thermal simulations are performed in the following step. Figures 7 and 8 present the thermal behaviour for the considered reinforced grid with 150 mm spacing. On the left side it is considerable that the temperature field is changed by using different heat conduction coefficient.

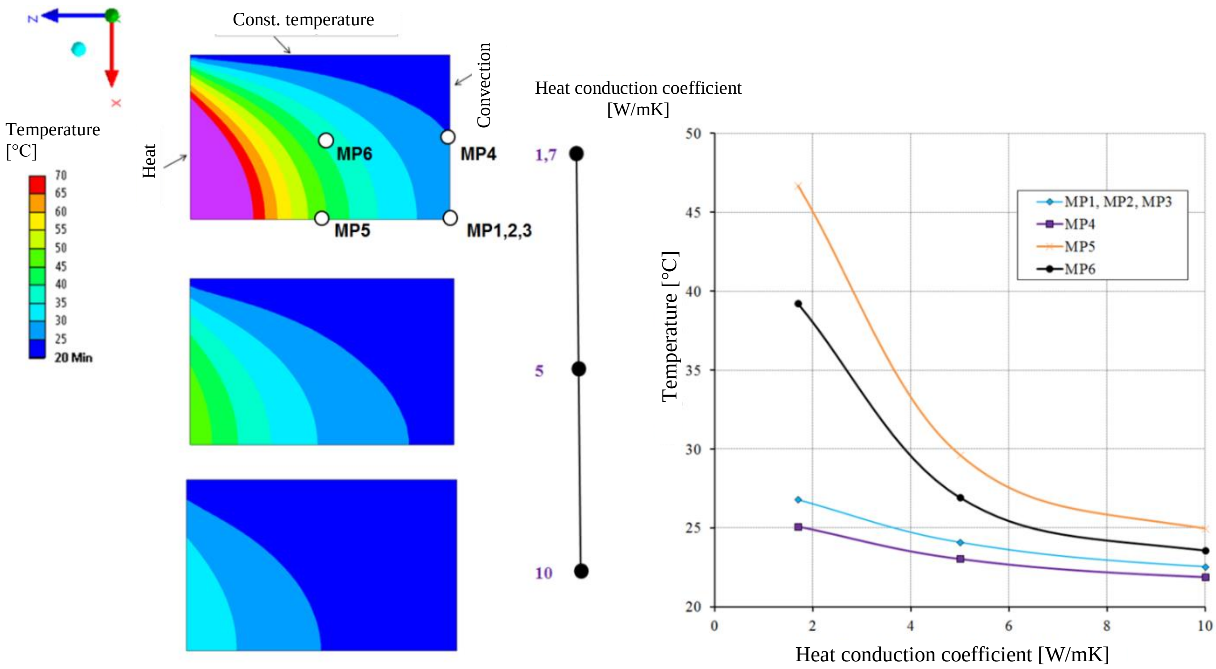

Fig. 6. Influence of the heat conduction coefficient on the temperature field

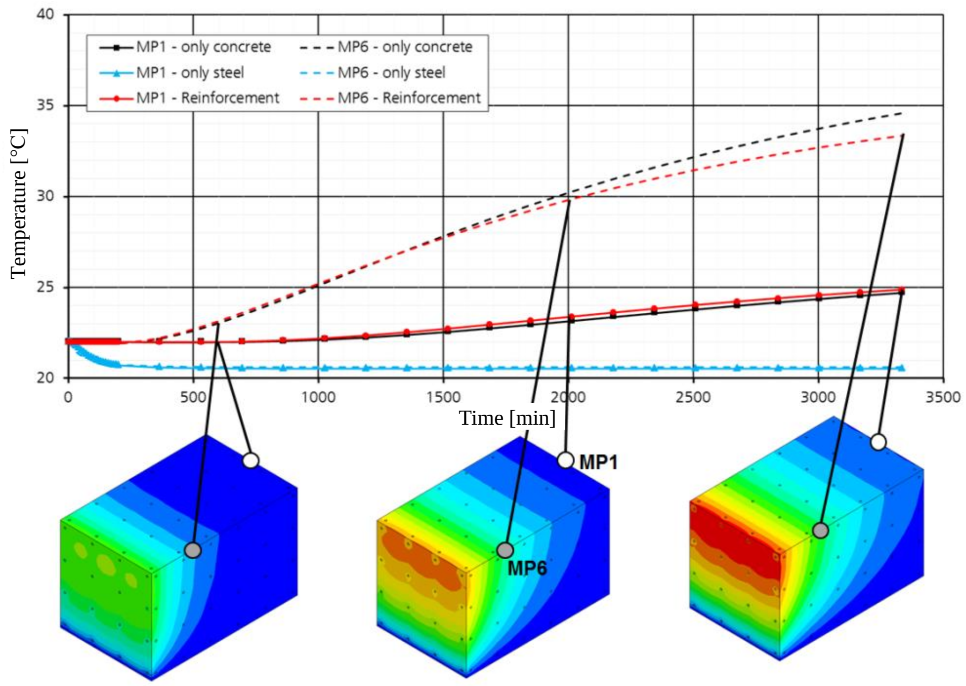

Fig. 7. Transient simulation of steel, concrete and reinforcement

The chosen range lies between 1.7 and 10 W/(mK). In comparison to the plotted temperature fields the trends of the heat conduction coefficient curves depending of the temperature distribution are mapped in the diagram on the right side of Fig. 7. For the investigation of the heat conduction a steady state simulation is sufficient.

The results show the decreasing temperature in the measurement points MP1 and MP6 by using higher heat conduction coefficients. This can be explained by a better heat conduction. The resulting context is also shown with the transient simulation (see Fig. 8). The steel reinforcement improves the heat conduction in a slightly way.

The heat conduction coefficient has been modified in the following steps, until a minimal difference between the reference values has been reached (see Fig. 9). For this case a parametric study in the Ansys 18.1 Workbench has been done. In the first step the heat conduction coefficient is increased from 1.7 W/(mK) up to 5 W/(mK) with a step size of 0.1 W/(mK).

Values Reinforced Model

Spacing reinforcement	only steel	(50 mm) 1)	(100 mm) 2)	(150 mm) 3)	(200 mm) 4)	only concrete
Elements:	111442	1298105	516456	385224	257347	111442
Nodes:	20558	382723	141840	100528	62919	20558
Calculation time [s]:	8	409	69	49	27	8
Measurement points			[°C]			
MP1	20.532	24.795	26.103	26.421	26.759	26.788
MP2	20.532	24.782	26.086	26.453	26.676	26.79
MP3	20.532	24.78	26.089	26.456	26.678	26.79
MP4	20.39	23.916	24.253	24.681	25.332	25.092
MP5	20.855	33.516	40.967	42.977	45.107	46.686
MP6	20.615	29.935	35.162	36.392	38.138	39.21
Volume reinforcement [m³]:	0.2	0.013974	0.0044295	0.0027545	0.001457	0
Volumen concrete [m³]:	0	0.186	0.196	0.197	0.199	0.2
Volume fraction reinforcement[%]:	100	6.987	2.215	1.377	0.729	0

							(for 100 mm)						(for 150 mm)						(for 200 mm)					
Heat Transfer Coefficient [W/(m*K)]	MP1	MP2	MP3	MP4	MP5	MP6	MP1	MP2	MP3	MP4	MP5	MP6	MP1	MP2	MP3	MP4	MP5	MP6	MP1	MP2	MP3	MP4	MP5	MP6
1.7	26.8	26.8	26.8	25.1	46.7	39.2	0.7	0.7	0.7	0.2	5.7	4.0	0.7	0.4	0.3	0.3	0.4	3.7	0.0	0.1	0.1	-0.2	1.6	1.1
1.8	26.7	26.7	26.7	25.0	45.3	38.2	0.6	0.6	0.6	0.1	4.3	3.0	0.6	0.2	0.2	0.2	0.3	2.3	-0.1	0.0	0.0	-0.3	0.2	0.1
1.9	26.5	26.5	26.5	24.9	44.0	37.3	0.4	0.4	0.4	0.0	3.1	2.1	0.4	0.1	0.1	0.1	0.2	1.0	-0.2	-0.1	-0.1	-0.4	-1.1	-0.8
2	26.4	26.4	26.4	24.8	42.9	36.5	0.3	0.3	0.3	-0.1	1.9	1.3	0.3	0.0	0.0	0.0	0.1	-0.1	-0.4	-0.3	-0.3	-0.5	-2.2	-1.7
2.1	26.3	26.3	26.3	24.7	41.9	35.7	0.2	0.2	0.2	-0.1	0.9	0.6	0.2	-0.1	-0.2	-0.2	0.0	-1.1	-0.5	-0.4	-0.4	-0.6	-3.3	-2.4
2.2	26.2	26.2	26.2	24.6	40.9	35.0	0.1	0.1	0.1	-0.2	-0.1	-0.1	0.1	-0.2	-0.3	-0.3	-0.1	-2.1	-0.6	-0.5	-0.5	-0.7	-4.2	-3.1
2.3	26.1	26.1	26.1	24.5	40.1	34.4	0.0	0.0	0.0	-0.3	-0.9	-0.7	0.0	-0.4	-0.4	-0.4	-0.1	-2.9	-0.7	-0.6	-0.6	-0.8	-5.1	-3.7
4.7	24.2	24.3	24.3	23.2	30.2	27.3	-1.9	-1.8	-1.8	-1.7	-10.8	-7.8	-1.9	-2.2	-2.2	-2.2	-1.5	-12.8	-2.5	-2.4	-2.4	-2.2	-14.9	-10.8
4.8	24.2	24.2	24.2	23.1	30.0	27.2	-1.9	-1.9	-1.9	-1.7	-11.0	-8.0	-1.9	-2.2	-2.3	-2.3	-1.6	-13.0	-2.6	-2.5	-2.5	-2.2	-15.1	-10.9
4.9	24.1	24.1	24.1	23.1	29.8	27.1	-2.0	-1.9	-1.9	-1.8	-11.2	-8.1	-2.0	-2.3	-2.3	-2.3	-1.6	-13.2	-2.6	-2.5	-2.5	-2.3	-15.3	-11.1
5	24.1	24.1	24.1	23.0	29.6	26.9	-2.0	-2.0	-2.0	-1.8	-11.3	-8.2	-2.0	-2.3	-2.4	-2.4	-1.6	-13.3	-2.7	-2.6	-2.6	-2.3	-15.5	-11.2

Fig. 8. Iterative determination of a modified heat conduction coefficient, step 1

After the first step there is established a new interval limit for the next iteration step with a refinement of the step size of 0.01. Usually two iterations are enough to get an adequately precise approximation of the heat conduction coefficient. After the second iteration a modified heat conduction coefficient of 1.99 to 2 W/(mK) for a homogeneous solid body can be detected in the second table of Fig. 9. For the evaluation criteria the average of the residual error for each point MP in comparison with the reinforced model is a good option (compare Fig. 3 and 9). The method for the specific heat capacity is nearly the same but therefor it is used a transient simulation for each design point. A design point in ANSYS 18.1 means one independent simulation with a set value for the heat capacity or conductivity. The evaluation has to be done for the temperature trend over the time.

							Difference (for 150 mm)						
Heat Transfer Coefficient [W/(m*K)]	MP1	MP2	MP3	MP4	MP5	MP6	MP1	MP2	MP3	MP4	MP5	MP6	Average
1.9	26.53	26.53	26.53	24.89	44.01	37.28	0.10	0.07	0.07	0.21	1.03	0.89	0.40
1.91	26.51	26.51	26.51	24.88	43.89	37.19	0.09	0.06	0.06	0.20	0.91	0.80	0.35
1.92	26.50	26.50	26.50	24.87	43.77	37.11	0.08	0.05	0.05	0.19	0.79	0.72	0.31
1.93	26.49	26.49	26.49	24.86	43.65	37.03	0.07	0.04	0.03	0.18	0.68	0.63	0.27
⋮							⋮						
1.98	26.43	26.43	26.43	24.81	43.09	36.62	0.01	-0.03	-0.03	0.13	0.11	0.23	0.07
1.99	26.42	26.42	26.42	24.80	42.98	36.54	-0.01	-0.04	-0.04	0.12	0.00	0.15	0.03
2	26.40	26.40	26.40	24.79	42.87	36.46	-0.02	-0.05	-0.05	0.11	-0.11	0.07	-0.01
2.01	26.39	26.39	26.39	24.79	42.76	36.38	-0.03	-0.06	-0.06	0.10	-0.22	-0.01	-0.05
2.02	26.38	26.38	26.38	24.78	42.66	36.31	-0.04	-0.07	-0.08	0.10	-0.32	-0.09	-0.08
⋮							⋮						
2.08	26.31	26.31	26.31	24.72	42.04	35.86	-0.11	-0.14	-0.15	0.04	-0.94	-0.53	-0.31
2.09	26.30	26.30	26.30	24.71	41.94	35.79	-0.12	-0.16	-0.16	0.03	-1.04	-0.60	-0.34
2.1	26.29	26.29	26.29	24.70	41.84	35.72	-0.14	-0.17	-0.17	0.02	-1.14	-0.67	-0.38

Fig. 9. Iterative determination of the adjusted thermal heat transfer, step 1

5. TRANSFER THE DEVELOPED METHOD TO A REAL MACHINE FRAME

The transfer of the approximation approach is carried out on a real machine frame, which consists of concrete and steel reinforcement. Figure 11 shows the steel reinforcement during the production process before the concrete come into the wood form. The function of the reinforcement is to stabilize the static behaviour of the machine frame. Inside the machine frame six independent cooling circuits and temperature sensors for a thermo-stabile structure behaviour is integrated. The research goal of the transfer project T02 as part of the CRC TR96 is to develop a decentral controlled tempering concept for thermo-stabile machine frames and structures. The whole demonstrator machine inclusive the mobile parallel kinematic is pictured in Fig. 12. In this paper the focus lies only in the investigation of the material behaviour of the composite material concrete and steel ratio. The measurement of the machine frame amounts circa 5 × 3 m and has a weight of 18 t. This machine frame has a big size and a sluggish thermal behaviour.

The machine frame can be separated in three areas referenced to the surface: area for the guide rails, area for the chip transport and an area of the stringboard with the inclusion of the processing unit. The processing unit is a 5-axis parallel kinematic milling machine of the company *METROM*.

The machine table is positioned on the guide rails and can be driven in a linear direction. Between the guide rails and the stringboard a canal is placed with a transport slug for the chips.

Fig. 10. Steel reinforcement in concrete

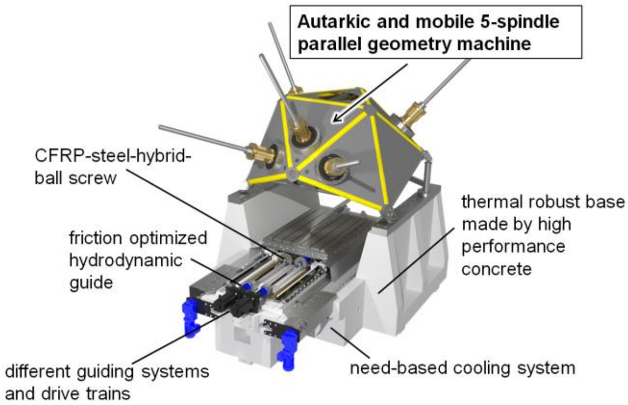

Fig. 11. Machine frame with processing unit

The two main motors for the drive of the machine table are placed frontal on a water-cooled flange. The other four cooling circuits are placed nearly the chip canal and the guiding rails to lead heat fluxes away quickly. For the experiments and verifying of the FE-simulation of the machine frame the cooling circuits have a warming function, because the influence of the heat conduction effects could be better displayed.

An analysis of the picture results in a simplified structure of the reinforcement with closely equidistant spacing of 150 mm. Figure 12 shows the influence of the reinforcement in the calculation time and the body properties.

As part of a transfer project T02 in SFB/Transregio 96 there have been performed experimental measurements by using the integrated cooling system. The aim of these investigations is to reach a steady temperature field in the machine frame and to verify the simulated influence of the fluid-cooling system by FEM. Each cooling circuit has a volume flow rate of 8 l/min and a warmed inlet temperature of 42°C.

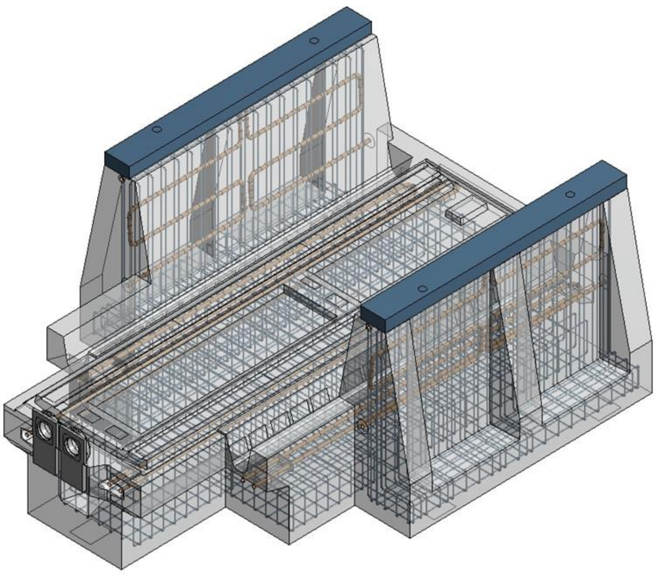

	without Reinforcement	with Reinforcement	Increasement Factor
Elements:	640333	3991181	6.233
Nodes:	208703	1042475	4.995
Calculation time			
Thermal simulation			
Calculation Time [min]	3.183	40.180	12.6
Use of memory [GB]	4.114	27.686	6.7
Mechanical displacement simulation			
Calculation Time [min]	4.217	52.450	12.44
Use of memory [GB]	9.229	29.608	3.21
Body properties			
Mass Reinforcement [kg]	306.470		
Volume Reinforcement [m³]	0.039		
Volume HPC (with Reinforcement) [m³]	7.102		
Mass HPC (with Reinforcement) [kg]	18464.000		
Volume HPC (without Reinforcement) [m³]	7.063		
Mass fraction [%]	1.642		

Fig. 12. Implementation of the steel reinforcement in the 3D-Volume body

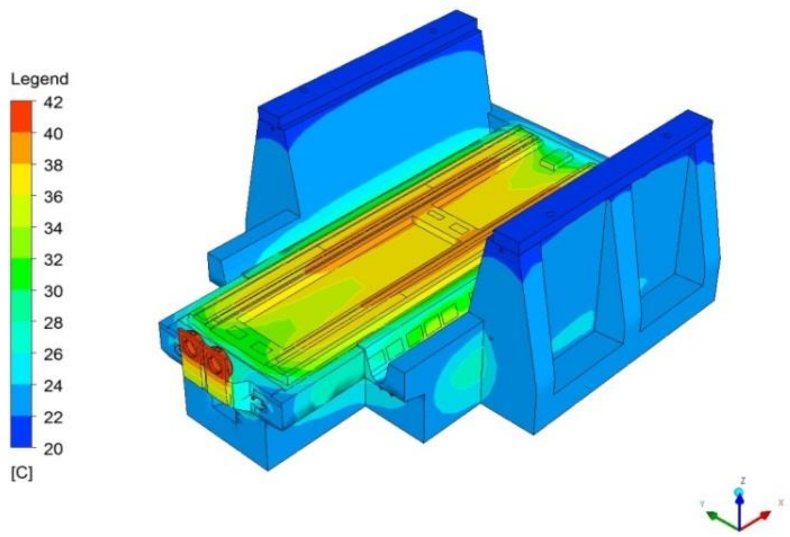

Fig. 13. Temperature field in the steady state

Inside the whole volume of the machine frame 23 temperature sensors are integrated. After nearly 60 hours a steady state of the temperature field could be detected. In the Fig. 13 the temperature distribution in the steady state can be recognized after the energetically balance between the convection with the environment and the heat sources.

In the following is described the comparison of the simulated temperature trend with measurement data trend on chosen sensor positions. The reference measurement point T1 is exactly in the middle of the machine frame and is not influenced by environmental effects. Because of this aspect and the wide distance from the cooling circuits is this point T1 an ideal indicator for the effects of the pure heat conduction. In the Figs 14 and 15 show the result of the comparison between the measurement and the simulation data. The left diagram presents the standard material data for the concrete from the material database of Ansys 18.1, the right diagram is calculated by using the modified material data.

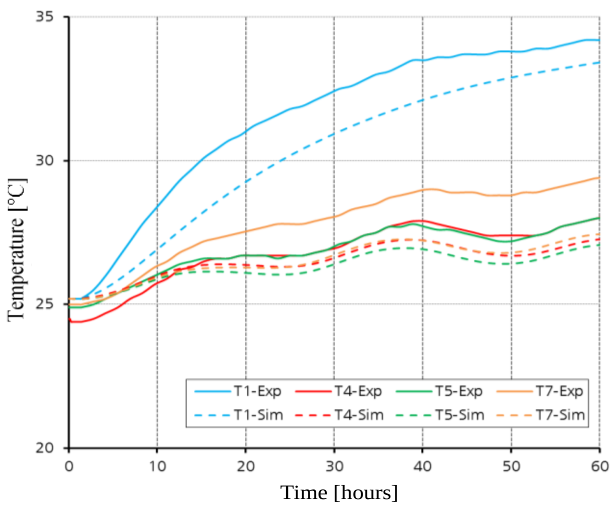

Fig. 14. Comparison simulation – experiment without modified material data

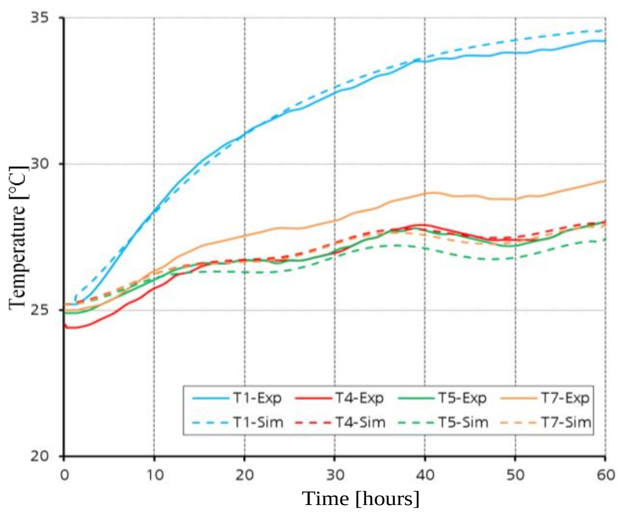

Fig. 15. Comparison simulation – experiment with modified material data

The direct comparison of the simulation and the experimental data shows a clear improvement due to the agreement with the data of the temperature sensors inside the machine frame by adjusted material data. Especially the reference measurement point T1 shows a great improvement (blue line). The new material data are determined iteratively with the method mentioned in Chapter 3 and represented in Table 3 in comparison with the following standard data for concrete.

Table 3. Representation of the material data

	Specific heat capacity [J/(kgK)]	Heat conduction coefficient [W/(mK)]
Standard material data	900	1.7
modified material data	730	1.99

The reinforcement can be considered on a reduced calculation model due to its simple structure. The two main influence factors of the heat equation, the heat conduction and the specific heat capacity, could be modified. This doesn't increase the calculation time, but improves the results obviously.

6. CONCLUSION

Beside the adoption of wrong boundary conditions, faulty material data are the most common source for simulation errors. That's why it is important to engage with set material data next to the choice of physically correct boundary conditions. Standard material data has to be questioned critically. Composites are generally a big challenge because of the non-linear influence of two or more materials. The methodical description in this article gives a procedure for the consideration of the reinforcement in concrete based on the simulation on a simplified model. To keep the calculation time for complex geometries low, expensive modelling strategies are not considered. The aim was to manipulate the material data in the simulation software for the solving of the heat conduction equations. Based on experimental measurement data this method could be verified successfully. The described method is not suitable for every issue, but on homogeneous reinforcement in a solid body with an equidistant spacing this method offers a good opportunity. Complex bodies can be separated in partial bodies to define material data for each part body independently.

Some resulting points can be summarized:

1) Reinforcement made of steel influences the thermal behavior of concrete, because the steel has a clear higher thermal conductivity and lower heat capacity.
2) Reinforcement with a spacing >250 mm can be neglect in common thermal analysis in most cases, because of a volume fraction much less than 1%. But not in strength analysis.
3) A volume fraction of 2.2% means a relative error of nearly 12%.
4) Simply and homogeneous constructed reinforcements can be well considered with reduced models and modified material data. But the method is not valid for strength characteristics.
5) More complex structures can be considered by separating in partial bodies with partial modified material data.

ACKNOWLEDGEMENTS

This research was supported by a German Research Foundation (DFG) grant within the Collaborative Research Centers/Transregio 96, which is gratefully acknowledged.

REFERENCES

[1] BRYAN J., 1990, *International status of thermal error research,* CIRP Annals – Manufacturing Technology, 39/2, 645–656.
[2] GROSSMANN K., et. al., 2015, *Thermo-energetic design of machine tools*, Lecture Notes in Production Engineering, Springer.
[3] DROSSEL W.-G., WITTSTOCK V., REGEL J., RICHTER C., NOFFKE F., 2014, *Auswirkungen lokaler Erwärmung von Mineralguss*, wt Werkstattstechnik Online, 104/9, 602–607.
[4] NEUGEBAUER R., DROSSEL W.G., IHLENFELDT S., NESTMANN S., RICHTER C., 2012, *Inherent thermal error compensation of machine tool structures with graded mineral casting*, International Conference on Machine Tools, Automation, Technology and Robotics. Prag, Czech Republic.
[5] WEBER J., GLÄNZEL J., POPKEN J., SHABI L., WEBER J., 2018, *Combined and Fast Computable Thermal Models for Situationally Optimal Tempering of Machine Components*, Institute of Fluid Power, TU Dresden, Fraunhofer Institute for Machine Tools and Forming Technology IWU, Chemnitz.
[6] HELLMICH A., GLÄNZEL J., IHLENFELDT S., 2018, *Methods for Analyzing and Optimizing the Fluidic Tempering of Machine Tool Beds of High Performance Concrete*, CIRP Conference on Thermal Issues in Machine Tools, Dresden.
[7] SCHNEIDER M., 2013, Das „intelligente“ Mineralgussbett, VDI-Z Integrierte Produktion, 155/3.
[8] DMG MORI SEIKI Schweiz AG, 2013, *Mehr Präzision für den Werkzeug- und Formenbau*, Technische Rundschau, KW 9.
[9] JUNG M., LANGER U., 2001, *Methode der finite Elemente für Ingenieure: Einführung in die numerische Grundlagen und Computersimulation*, TEUBNER – Stuttgart, Leipzig, Wiesbaden.